Development and characterization of active packaging films based on chitosan and sardinella protein isolate: Effects on the quality and the shelf life of shrimps

Youssra Ben Azaza, Marwa Hamdi, Christophe Charmette, Mourad Jridi, Suming Li, Moncef Nasri, Rim Nasri

Development and characterization of active packaging films based on chitosan and sardinella protein isolate: Effects on the quality and the shelf life of shrimps

Youssra Ben Azaza [a,*], Marwa Hamdi [a], Christophe Charmette [b], Mourad Jridi [a,c], Suming Li [b], Moncef Nasri [a], Rim Nasri [a,d]

[a] *Laboratory of Enzyme Engineering and Microbiology, University of Sfax, National Engineering, School of Sfax, P.O.B. 1173-3038, Sfax, Tunisia*
[b] *Institut Européen des Membranes, IEM, UMR 5635, Univ Montpellier, ENSCM, CNRS, Montpellier, France*
[c] *Higher Institute of Biotechnology of Beja, University of Jendouba, Beja, Tunisia*
[d] *Higher Institute of Biotechnology of Monastir, University of Monastir, P.O.B. 5000, Monastir, Tunisia*

Keywords:
Sardinella protein isolate
Chitosan
Composite films
Antioxidant properties
Shrimp packaging

The transformation of wastes from food processing industry to value-added products is one of the major challenges in sustainable development. This work aimed to develop active packaging films based on chitosan (Cs) and sardinella protein isolate (SrPI) obtained from blue crab and *Sardinella aurita by-products*, respectively. The data from fourier transform infrared (FTIR) spectroscopy, scanning electron microscopy (SEM), and thermogravimetric analysis (TGA) indicate an improvement in the structural and thermal properties of the films by incorporating SrPI into the chitosan matrix. In contrast, the composite films exhibited lower mechanical properties than the Cs film. Composite and Cs films were employed to package the shrimp in order to improve their conservation. The results showed that the increased SrPI content in packaging films improved the chemical properties and microbial stability of wrapped shrimps during cold storage. Therefore, these results encourage the use of Cs-SrPI films as active packaging material.

1. Introduction

Biopolymers have attracted much attention for developing new materials due to their outstanding physico-chemical, functional, film-forming and biological properties (Coltelli et al., 2015). Among these biopolymers, chitosan extracted from shells of crustaceans (Blue crab: *Portunus segnis*) and protein isolate extracted from by-products of round sardinella (*Sardinella aurita*) present interesting physico-chemical and biological properties. Chitosan (β-linked D-glucosamine and N-acetyl-D-glucosamine) is a polysaccharide obtained by deacetylation of chitin from the shell of crustaceans by chemical or microbiological processes (Hamdi et al., 2018). Chitosan is soluble in weakly acidic environments (pH < 6) due to its inherent cationic nature. Because of its biodegradability, biocompatibility, antimicrobial and antifungal activities, and filmogenic property, chitosan is used in a wide range of fields, including packaging, textile, agriculture, pharmaceuticals, electronics (Yang, 2011), and seafood product preservation (Mohan, Ravishankar, Lalitha & Srinivasa Gopal, 2012; Souza et al., 2010).

Marine by-products are considered as sources of raw materials to obtain biopolymers with outstanding properties. Currently, protein isolates are recovered from marine by-products by using the protein isolation method. These protein isolates can be utilized not only as a food additive, but also as a component in the preparation of film-forming materials for a variety of applications due to their high content of biological value and nutritional quality (Li et al., 2017).

Biofilms are biopolymer layers that function as a barrier to the flow of moisture, oxygen, carbon dioxide, and solutes in food. Biofilms degrade quickly because they are made entirely of renewable food materials including polysaccharides, gelatin, and fish myofibrillar proteins (Batista, Araújo, Peixoto Joele, Silva & Lourenço, 2019). As one of the most abundant polysaccharides, chitosan is widely used to prepare biofilms with very good gas barrier properties which allow to increase the shelf life of food products (van den Broek, Knoop, Kappen & Boeriu, 2015). However, there are several limits to the use of chitosan films. The most well-known disadvantage is that the chitosan film is very brittle and hard. Further, chitosan films are sensitive to moisture due to their

* Corresponding author.
E-mail address: youssra.benazaza@enis.tn (Y.B. Azaza).

hydrophilic nature (Niamsa, Morakot, & Baimark, 2010).

Recently, the application of films as edible coating has been shown to improve food safety and prevent contamination of food products through decomposition (Duan, Wu, Strik & Zhao, 2011).

The aim of this study was to develop composite films from chitosan (Cs)-sardinella protein isolate (SrPI) as edible packaging. The composite films were characterized using fourier transform infrared (FTIR), mechanical tests, thermogravimetric analysis (TGA), scanning electron microscopy (SEM), as well as moisture content (MC), water solubility (WS), and optical measurements. The antioxidant and antibacterial characteristics of composite films were evaluated. Furthermore, the effect of SrPI addition to the composite films on the quality and shelf-life of shrimps during refrigerated storage was assessed based on different chemical and microbiological parameters.

2. Materials and methods

2.1. Materials

Sardinella aurita and blue crab were purchased in fresh conditions from a fishery market located at Sfax City, Tunisia. Fresh shrimps, with a uniform average weight and no visible damage, were purchased from a local fish store in Sfax, Tunisia.

Glycerol was used as a plasticizer and purchased from Sigma-Aldrich. Acetic acid, hydrochloric acid (HCl), hexane, chloroform and methanol of reagent grade were purchased from Sigma Chemical Co. DPPH (2, 2-diphenyl-1-picrylhydrazyl), ferrozine (3-(2-Pyridyl)-5,6-diphenyl-1,2,4-triazine), ferrous chloride, ferrous ion, linoleic acid, potassium ferricyanide, trichloroacetic acid (TCA), sodium chloride (NaCl), ammonium thiocyanate, tris(hydroxyméthyl)aminométhane (Tris), butylated hydroxytoluene (BHT), and 2-thiobarbituric acid (TBA) were procured from Sigma Chemical Co. (St. Louis, MO, USA).

2.2. Sardinella protein isolate preparation

Protein isolate was extracted from *S. aurita* by-products as described by Nasri et al. (2020). At first, sardinella by-products were washed to remove impurities, and then cut into small pieces. Homogenization step was carried out with cold distilled water (4 °C) at a ratio of 1:10 (w/v) using an Ultra-turrax apparatus (IKA, T18 basic). The homogenate was adjusted to pH 11.0 using 1 M NaOH, stirred gently at room temperature for 18 h, and then centrifuged for 30 min at 4 °C at 8 000 rpm. The supernatant was precipitated at the nominal isoelectric point of 5.5 using 1 M HCl, and then centrifuged at 8 000 rpm for 30 min. Finally, 1 M NaOH was used to adjust the pH of the supernatant to 7.0. Afterwards, soluble proteins in supernatant were spray-dried on a rotary atomizer (BUCHI B-290, Arch Spray Drying Services, USA) at 170 °C inlet and 80 °C outlet temperatures and at 90% aspirator rate. SrPI, the resultant powder, was kept at 4 °C for further use. The yield of protein isolate recovery was calculated based on wet weight of fresh by-products.

Total nitrogen content, ash, moisture and dry matter content were determined using the AOAC method (AOAC, 2000). The fat content was estimated after Soxhlet extraction of dried sample with hexane for 2 h using Nahita Model 655, Navarra.

2.3. Chitosan preparation

Chitosan was prepared from blue crab shells (*Portunus segnis*) as described by Hamdi, Nasri, Li, and Nasri (2019). The blue crab shells were carefully separated, washed with tap water to remove impurities and heated for 20 min at 90 °C. Then, they were dried at room temperature and powdered in a Moulinex® blender. Demineralization was performed chemically in a solution of 0.55 M HCl at a ratio of 1/10 (w/v), using three repeated acid baths for a duration of 30 min per bath. Then, depoteinisation was performed using Purafect for 3 h with an enzyme/substrate ratio of 5 U/mg protein and under optimal enzymatic conditions (pH 10.0 and temperature 50 °C). Finally, chitin was converted to chitosan by processing with 12.5 M NaOH at a ratio of 1/10 (w/v) at 140 °C. After filtration, the residue was washed with distilled water until the pH was neutral, and the obtained chitosan was dried at 50 °C overnight. The degree of deacetylation (DD) and molecular weight (Mn) of the resulting chitosan was 90% (Hamdi et al., 2018) and 115, 000 g/mol (Hamdi, Nasri, Amor, Li, Gargouri & Nasri, 2020), respectively.

2.4. Composite films preparation

For the production of the films, chitosan (2%, w/v) was mixed with varied quantities of SrPI (2%, w/v). Final solutions with various volume ratios of Cs-SrPI (100:0, 90:10, 80:20, 70:30, 60:40 and 50:50) were gently mixed for 15 min at room temperature. Then, as a plasticizer, 15% (w/w compared to Cs) of glycerol was added. Following this, 25 mL of the prepared solution was poured into a plastic petri dish and then dried at room temperature for 48 h. Dried films were peeled off and then stored at room temperature and a relative humidity (RH) of 50%. The obtained composite films were designated as Cs90–10SrPI, Cs80–20SrPI, Cs70–30SrPI, Cs60–40SrPI and Cs50–50SrPI. Pure chitosan (Cs100) films were prepared as control.

2.5. Film characterization

2.5.1. Moisture content and water solubility

Moisture content (MC) of the films was determined by drying approximately 100 mg of each sample in an oven at 105 °C up to constant weight. The MC of films is expressed as g moisture / 100 g dry solid.

Water solubility (WS) was assessed as the percentage of dry matter of the film solubilized in water during a period of 24 h according to Gennadios, Handa, Froning, Weller, and Hanna (1998). Tests were performed in triplicate.

2.5.2. Ultraviolet-visible spectroscopy and opacity

The transmittance spectra of the prepared films were registered using a UV–visible spectrometer (T70, UV / Vis spectrometer, PG Instruments Ltd., China) in the wavelength range from 200 to 800 nm. The percentage light transmittance was measured at 280 nm (T280) and 660 nm (T660) to evaluate UV-barrier property and opacity, respectively. The opacity of the films was calculated by using the following equation:

$$Opacity = \frac{A_{600}}{e} \quad (1)$$

where A_{600} is absorbance at 600 nm, and e is the film thickness (mm).

2.5.3. Color properties

The color parameters L^* (lightness), a^* (redness/greenness), b^* (yellowness/blueness) of films were evaluated using a CR-5 colorimeter Konica Minolta (Sensing Europe B.V). The total color difference ($\triangle E$) was calculated as follows:

$$\triangle E* = [(\triangle L^*)^2 + (\triangle a^*)^2 + (\triangle b^*)^2]^{1/2} \quad (2)$$

2.5.4. Mechanical properties and thickness of films

The elongation at break (EAB, %) and tensile strength (TS, MPa) of Cs and Cs-SrPI films were measured using a Physica MCR rheometer (Anton Paar, GmbH, France) according to ISO standard. Prior to analysis, all films were equilibrated for two weeks at 25 °C and 50% RH and then cut into rectangles (1.0 cm × 4.5 cm). The samples were subjected to a uniaxial tensile test up to breakage at a strain rate of 5 mm/min. The EAB and TS values were obtained from the corresponding stress-strain curves. At least six duplicate measurements were made for each sample at room temperature (25 ± 2 °C).

The thickness of samples was measured using a micrometer

(Digimatic IP65, Mitutoyo, France) with an accuracy of 1 μm. Five random measurements were recorded from each sample at different positions (center and perimeter).

2.5.5. Fourier transform infrared (FTIR) analysis

The FTIR spectra of Cs-SrPI films were registered employing a spectrometer (Agilent Technologies, Carry 630 series) equipped with an attenuated reflection accessory (ATR) containing a diamond/ZnSe crystal. 32 scans were recorded at room temperature (25 ± 2 °C) within the wavenumber range of 4000–400 cm^{-1}.

2.5.6. Water vapor permeability (WVP)

The *WVP* measurements of films were evaluated using the modified ASTM E96–95 standards. The film samples (75 mm × 75 mm) were conditioned at 25 °C and 50% RH for a minimum equilibration time of 48 h. Films were mounted on top of the *WVP* cup (depth = 25 mm; diameter = 68 mm) containing 15 mL distilled water and sealed completely. The *WVP* cup was placed in a humidity chamber (KBF 240 Binder, ODIL, France). Under constant conditions of 25 °C and an RH of 50%, the weight of samples was recorded at 1 h intervals for 10 h. The films' thickness was measured, and the *WVP* (g m^{-1} s^{-1} Pa^{-1}) was calculated:

$$WVP = \frac{\Delta w * e}{A * \Delta t * \Delta P} \quad (3)$$

where Δw is the weight variation of the cup (g); e is the film thickness (m); A the exchange surface of the film exposed to water vapor transfer (1.39×10^4 m^2); Δt is the time of weight variation (s); ΔP (P2-P1) is the partial vapor pressure differential across the film (Pa). All films were measured three times.

2.5.7. Film's microstructure

The film cross-section morphology was visualized employing Hitachi S4800 scanning electron microscope, at an accelerating voltage of 2.0 kV and pressure absolute of 60 Pa. After attaching the film pieces on SEM support, samples were cryofractured by immersion in liquid nitrogen, then observed.

2.5.8. Thermal properties of composite films

Thermogravimetric analysis (TGA) was performed using TGAQ 500 instruments (TA Instruments). The samples are heated from 25° to 700°C at a rate of 20 °C/min.

2.6. Biological activities evaluation

2.6.1. Antioxidant activity of composite films

2.6.1.1. DPPH free radical-scavenging assay. The DPPH radical-scavenging activity of films (10 mg) and SrPI solutions (1–4 mg/mL) was determined according to the method of Bersuder, Hole, and Smith (1998) with slight modifications. Samples were immersed in 375 μL of ethanol, followed by addition of 125 μL of 0.02% DPPH (in ethanol) as free radicals' source. The obtained mixture was homogenized and incubated for 24 h at 25 °C in the dark. The reduction of DPPH radicals was measured at 517 nm (T70, UV/Vis spectrometer, PG Instruments Ltd., China). Hydroxyanisole butyl (BHA) was used as a positive control. DPPH radical scavenging activity was calculated as follows:

$$\text{Radical scavenging activity } (\%) = \frac{[A_c + A_b - A_S]}{A_c} \; x \; 100 \quad (4)$$

where A_c, A_b, and A_s represent the absorbance of the control (containing all reagents except the sample), the blank (containing all reagents except the DPPH solution), and the composite films with the DPPH solution, respectively.

2.6.1.2. Metal chelating activity. The iron chelating effect of Cs-SrPI films (10 mg) and SrPI solutions (0.25–1 mg/mL) towards ferrous ion (Fe^{2+}) was studied as reported by Decker & Welch (1990). Samples were mixed with 450 μL of distilled water. Then, 50 μL of 2 mM $FeCl_2$ and 200 μL of 5 mM Ferrozine (3-(2-Pyridyl)-5,6-bis(4-phenylsulfonic acid)-1,2,4-triazine) were added. The reaction mixture was vigorously stirred and incubated for 20 min at room temperature (25 ± 2 °C). EDTA was used as a reference. The chelating activity (%) was calculated as follows:

$$\text{Metal chelating activity } (\%) = \frac{[A_c + A_b - A_S]}{A_c} \; x \; 100 \quad (5)$$

where A_c, A_b, and A_s represent the absorbance of the control, the blank and the samples, respectively. The test was carried out in triplicate.

2.6.1.3. Reducing power assay. The ability of Cs-SrPI films and SrPI solutions to reduce iron was determined according to the method of Yildirim, Mavi, and Kara (2001), with minor modifications. Film samples (10 mg) and SrPI solutions (1–4 mg/mL) were immersed in a mixture of 1.25 mL of 0.2 M phosphate buffer (pH 6.6) and 1.25 mL of potassium ferricyanide (1%, w/v), and incubated for 30 min at 50 °C. 1.25 mL trichloroacetic acid (10%, m/v) was then added to the mixture in order to stop the reaction. Finally, the mixture was centrifuged for 10 min at 3 500 g, and the supernatant (1.25 mL) was mixed with 1.25 mL distilled water and 0.25 mL ferric chloride (1%, m/v). The absorbance of the resulting solution was measured at 700 nm after 10 min incubation. BHA was used as a standard. Three replicates were performed for each test sample.

2.6.1.4. β-carotene bleaching method. The prevention of β-carotene from bleaching of films (10 mg) and SrPI solutions (1–4 mg/mL) was determined according to the method of Koleva, van Beek, Linssen, de Groot, and Evstatieva (2002). Tests were carried out in triplicate and the antioxidant activity was evaluated in terms of β-carotene bleaching using the following equation:

$$\beta - \text{carotene bleaching } (\%) = \frac{[1 - (A_0 - A_t)]}{[A_0' - A_t']} \; x \; 100 \quad (6)$$

where A_0 and A_t are the absorbance of the test sample measured before and after incubation, respectively; and A_0' and A_t' are the absorbance of the control measured before and after incubation, respectively.

2.6.2. Antibacterial activity

The antibacterial activity of the chitosan and composite film solutions was evaluated according to the agar diffusion method described by Van Den Berghe, Ieven, Mertens, and Vlietinck (1978). 5 Gram-negative bacteria and 4 Gram-positive strains were tested, i.e *Salmonella enterica* (ATCC 43972), *Pseudomonas aeruginosa* (ATCC 15442), *Enterobacter sp, Escherichia coli* (ATCC 4698), *Klebsiella pneumoniae* (ATCC 13883), *Staphylococcus aureus* (ATCC 25923), *Micrococcus luteus* (ATCC 4698), *Listeria monocytogenes* (ATCC 13932) and *Bacillus cereus* (ATCC 11778). First, the examined strains' culture suspensions were dispersed over Muller-Hinton agar medium. The film solutions were then placed into wells in the agar with 60 μL in each well. After a 24-hour incubation period at 37 °C, the antibacterial activity was measured by measuring the diameter of the growth inhibition zone around the wells (including well diameter of 6 mm).

2.7. Application of films in shrimp preservation

2.7.1. Edible packaging of shrimp preparation

Fresh shrimps, with average weight (5 g) and no visible damage, were purchased from a local fish store in Sfax, Tunisia. In order to determine the effects of Cs and SrPI films during storage, purchased

shrimps were pretreated by washing with running water and peeled aseptically with a sterile surgical scalpel. The shrimps were randomly divided into four groups, 2 shrimps in each group. The groups were referred as follows: (SH-C) control shrimp (unpackaged); (SH-1) shrimp packaged with the Cs100 film; (SH-2) shrimp packaged with Cs90–10SrPI film, and (SH-3) shrimp packaged with Cs50–50SrPI film. The various groups were then aseptically covered with the films and stored in a refrigerator (4 ± 1 °C). To simulate realistic storage conditions, only the top part of the shrimp that was in close contact with the films was analyzed after 0, 3, 6, and 9 days of storage at 4 °C. Different properties of samples were evaluated, including moisture content, pH value, thiobarbituric acid reactive substance (TBARS), conjugated dienes, and peroxide content. Microbiological analysis was also performed. Three replicates per treatment were used for each sampling time.

2.7.2. Chemical evaluation

The moisture content was determined after evaporating the water contained in 5 g of sample at 105 °C during 24 h (AOAC, 2000).

For pH measurement, 5 g of the samples were homogenized with 10 mL of distilled water. After remaining 5 min at room temperature, the pH of samples was determined using a pH-meter (Volpe et al., 2015).

2.7.3. Determination of peroxide value

The peroxide value (PV) was determined following the method of Shantha & Decker, (1993), with some modifications. The sample (0.5 g) was mixed with 16.3 mL chloroform–methanol in a glass tube, and vortexed for 2–4 s. Ammonium thiocyanate solution (10 mM) (0.08 mL) was added, and the sample was vortexed for 2–4 s. Then, 0.08 mL iron (II) solution was added, and the sample was vortexed for 2–4 s. Finally the mixture was incubated for 5 min at room temperature. and the absorbance was measured at 500 nm. PV was expressed as milli-equivalents of peroxide oxygen combined in a kilogram of fat.

2.7.4. Determination of thiobarbituric acid reactive substances

The thiobarbituric acid reactive substances (TBARS) test was determined according to the procedure of Buege & Aust (1972), with some modifications. In brief, shrimp samples (0.5 g) were homogenized with 625 µL of TBS (50 mM Tris containing 150 mM NaCl, pH 7.4) and 375 µL of TCA/BHT (TCA 20%, BHT 1%) in order to precipitate proteins. The homogenates were then centrifuged (1000 g, 10 min, 4 °C) and the supernatant was used for TBA test. Aliquots of 400 µL of each supernatant were mixed with 80 µL of HCl (0.6 M) and 320 µL of Tris/TBA (Tris 26 mM; TBA 120 mM), and heated in boiling water bath for 10 min. The mixed solutions were cooled down to room temperature. The absorbance of the resulting solutions was measured at 530 nm. The results were expressed as milligram of malonaldehyde equivalents per kilogram of sample.

2.7.5. Determination of the conjugated dienes content

Lipid oxidation was also assessed from the conjugated diene content using the method of Srinivasan, Holl, and Petersen (2011). 3.0 g sample was suspended in 30 mL distilled water, and homogenized to form a "smooth slurry". 3 mL aliquot of this suspension was mixed with 30 mL extracting solution (3:1 hexane: isopropanol) for 1 min. After 5 min centrifugation at 2000 g, the absorbance of the supernatant was read at 233 nm.

2.7.6. Microbiological analysis

A shrimp sample of 1 g was homogenized with 9 mL of 0.9% NaCl solution at room temperature. A series of dilutions were prepared from this solution. The total psychrophilic flora (TPF) and the total mesophilic flora (TMF) were estimated after incubation of the dilutions in plat count agar (PCA) medium for 48 h at 37 °C and for 7 days at 4 °C, respectively. All microbial counts were converted to logarithms of colony-forming units per gram of shrimp sample (log CFU/g).

2.8. Statistical analysis

All the experiments were realized in triplicate, based on the test used. The average values with the standard deviation error were reported. Statistical analyses were analyzed using SPSS ver. 20.0 professional edition (SPSS, Inc., Chicago, IL, USA) via ANOVA analysis. Differences were considered significant at $p < 0.05$.

3. Results and discussion

3.1. Characterization of Sardinella protein isolate

3.1.1. Chemical analysis of SrPI

The chemical composition of spray-dried SrPI produced by the pH-shifting technique is shown in Table S1 (Supplementary data). The yield extraction of SrPI was 19.8% which was slightly higher than that of crab blue muscle protein isolate (18.4%) (Hamdi, Feki, et al., 2020), but lower than that of lanternfish protein isolate (31.3%) (Oliyaei, Ghorbani, Moosavi-Nasab, Sadeghimahoonak & Maghsoudloo, 2017). Results show also that SrPI contains high protein content (81.3%) and low contents of moisture (5.0%), ash (9.5%) and fat (2.6%). Kumarakuru, Reddy, and Haripriya (2018) reported that sardine protein isolate obtained by alkaline solubilization and acid precipitation had a high protein concentration and low moisture, ash, and fat levels. In another work, Taktak et al. (2019) reported also that the recovered European eel protein isolate contained high amount of protein (94 g/100 g) and low amount of fat (3.4 g/100 g).

3.1.2. Antioxidant activities of SrPI

The determination of a single antioxidant mechanism would not be sufficient to assess the overall antioxidant potential of biomaterials. SrPI was analyzed using various in vitro antioxidant tests including reducing power, ferrous ion-chelating activity, DPPH radical-scavenging activity, and β-carotene linoleic acid bleaching method.

The results of the reducing power, presented in Supplementary data (Fig. S1A), indicated that SrPI exhibited an interesting reducing power of 3.0 at 4 mg/mL. A positive correlation between the SrPI concentration and its reducing power was observed. Cho (2020) reported a reducing power of 0.525 at 4 mg/mL for rice bran protein isolate, which is lower than that of SrPI. These findings indicated that SrPI is an effective electron donor for free radicals.

On the other hand, SrPI showed an interesting metal chelating effect, reaching 100% at a concentration of 0.5 mg/mL, which is comparable to EDTA at all concentrations (Fig. S1B). It is suggested that SrPI could be used as a chelating agent in food applications, promoting the prevention of peroxidation and thus avoiding food spoilage (Nasri et al., 2013).

Furthermore, as shown in Fig. S1C, the antiradical activity of SrPI on DPPH radical increased with increasing concentration. Nevertheless, the antioxidant activity of SrPI didn't exceed 21% at a concentration of 4 mg/mL.

The results of the β-carotene bleaching test showed that SrPI exhibited a dose-dependent scavenging capability of linoleate free radicals (Fig. S1D). Unlike the DPPH test, the β-carotene bleaching test was performed in an emulsion medium. Hence, SrPI is more effective against lipophilic radicals (linoleic radical) than against hydrophilic radicals (DPPH radical).

3.2. Characterization of composite films

3.2.1. Moisture content and water solubility of composite films

The effect of adding SrPI to Cs-based films on moisture content was evaluated, and the findings are presented in Table 1. Control film Cs100 had the lowest MC values of 15.80% ($p < 0.05$), while composite films showed significantly higher MC values ranging from 25% to 31.45%. Hence, data revealed that the polymeric interaction between myofibrillar proteins and chitosan improves the water retention in their

Table 1
Moisture content (MC), water solubility (WS), water vapor permeability (WVP), thickness, mechanical properties and antioxidant activities of composite films.

Films	Cs100	Cs90-10rSPI	Cs80-20SrPI	Cs70-30SrPI	Cs60-40SrPI	Cs50-50SrPI
MC (%)	15.80 ± 0.37^{a}	25.00 ± 1.03^{b}	29.78 ± 0.34^{c}	26.75 ± 1.63^{b}	31.45 ± 1.83^{d}	29.65 ± 0.13^{c}
WS (%)	31.64 ± 1.10^{a}	38.04 ± 1.20^{b}	47.35 ± 0.35^{c}	55.88 ± 0.63^{d}	57.15 ± 0.92^{d}	57.25 ± 0.78^{d}
WVP ($g{\cdot}s^{-1}{\cdot}m^{-1}{\cdot}Pa^{-1}$ x 10^{-10})	4.26 ± 0.01^{f}	4.18 ± 0.08^{e}	3.81 ± 0.00^{d}	3.71 ± 0.06^{c}	3.26 ± 0.08^{b}	3.11 ± 0.05^{a}
Thickness (μm)	38.65 ± 1.83^{a}	40.50 ± 1.00^{ab}	41.80 ± 4.32^{ab}	47.25 ± 4.27^{c}	49.25 ± 2.87^{d}	50.33 ± 3.06^{e}
TS (MPa)	19.13 ± 0.68^{e}	17.85 ± 0.49^{d}	17.57 ± 0.29^{d}	16.82 ± 0.53^{c}	13.58 ± 0.36^{b}	10.05 ± 0.69^{a}
EAB (%)	25.02 ± 3.01^{f}	23.52 ± 0.84^{e}	18.35 ± 0.24^{d}	15.68 ± 0.13^{c}	13.49 ± 0.90^{b}	8.74 ± 0.58^{a}
DPPH Radical Scavenging activity	74.1 ± 0.58^{a}	98.18 ± 0.52^{b}	98.42 ± 0.34^{b}	100 ± 0.00^{c}	100 ± 0.00^{c}	100 ± 0.00^{c}
Ferrous reducing ability (OD_{700})	0.165 ± 0.009^{a}	0.37 ± 0.00^{b}	0.512 ± 0.005^{c}	0.59 ± 0.00^{d}	0.72 ± 0.00^{e}	0.894 ± 0.008^{f}
Metal chelating effect (%)	36.00 ± 0.02^{a}	65.38 ± 0.55^{b}	70.24 ± 0.89^{c}	77.86 ± 0.44^{d}	79.62 ± 0.53^{e}	84.07 ± 2.56^{f}
β-carotene bleaching inhibition (%)	23.21 ± 0.85^{a}	25.19 ± 0.58^{b}	45.59 ± 0.81^{c}	51.46 ± 0.04^{d}	53.22 ± 0.48^{e}	54.17 ± 0.57^{f}

Results are the means of three determinations ± standard deviation. [a-f] Different letters in the same column indicate a significant difference ($p < 0.05$). **SrPI**: sardine protein isolate; **Cs**: blue crab chitosan.

network.

Moreover, the water solubility of different samples was evaluated. As shown in Table 1, the increase of SrPI concentration increased considerably the WS level of composite films ($p < 0.05$), which could notably impact their barrier properties. Indeed, Cs50–50SrPI film achieved the highest WS (57.25%), while Cs100 film presented the lowest WS (31.64%). It is well known that chitosan is completely soluble only in an acidified aqueous solution which explains the low solubility of Cs films. Subsequently, the addition of the proteins in the film-forming matrix allowed reducing the resistance of the biofilms to water. According to Hosseini, Rezaei, Zandi, and Ghavi (2013), the development of intermolecular interactions between biopolymers is responsible for the improved solubility of chitosan-gelatin-based films. Solubility fluctuation on polymer-based films could be caused by electrostatic forces and hydrogen bonding. Jridi et al. (2014) obtained higher solubility for chitosan film (50.35%) than in the present study, which could be related to the much lower Mn (17,030 g/mol) of chitosan.

3.2.2. *Water vapor permeability of composite films*

WVP determines the ability of an edible film to counteract the water loss of the product due to environmental exposure, and also to resist atmospheric moisture. A low WVP of the film is preferred in packaging material. Table 1 shows the WVP of Cs and Cs-SrPI film samples. The Cs100 film present a high WVP due to its hydrophilic character. For composite films, a decrease of WVP value from 4.18 g s^{-1} m^{-1} Pa^{-1} x 10^{-10} for Cs100 to 3.11 g s^{-1} m^{-1} Pa^{-1} x 10^{-10} for Cs50–50SrPI ($p < 0.05$) was noted. These findings suggest that incorporating SrPI might increase the cross-linking degree in Cs100 film, restrict the movement of polymer chains, and prevent, thereby, the penetration of water vapor (Anuar et al., 2017; Shen, Wu, Chen & Zhao, 2010). Hence, SrPI can improve the moisture barrier performance, which is critical for improved packaging applications. Samsalee & Sothornvit (2019) also reported the same trend in the WVP values of porcine plasma protein-chitosan films.

3.2.3. *Thickness and mechanical properties of composite films*

The thickness values of the composite films are shown in Table 1. Data reveal that thickness ranged from 38.65 to 50.33 μm ($p < 0.05$). Besides, the composite films were thicker than Cs100 film (38.65 μm). The increase in the thickness of composite films may be related to the amount and the nature of polymers added to the film formulation (García & Sobral, 2005). These findings are consistent with those of Hamdi et al. (2019) and Hamdi, Nasri, Hajji, et al. (2019), who found that the chitosan film thickness was much lower than that of cartenoprotein-enriched chitosan films.

The most important mechanical parameters to packing material are TS and EAB. Table 1 lists the mechanical parameters of Cs100 and Cs-SrPI films. Cs100 film had the highest EAB (25%) and TS (19.3 MPa) values. The addition of SrPI reduced the TS and EAB of composite films in a dose-dependent manner. Cs50–50SrPI film presents the lowest EAB (8.74%) and TS (10.05 MPa) values. Zhang et al. (2019) and Samsalee & Sothornvit (2019) found that including a high amount of protein (zein and porcine plasma protein, separately) to the chitosan film matrix decreased the TS and EAB values of blended films. The decrease in mechanical parameter's values could be essentially attributed to a distortion of the film network (polysaccharides-protein) due to the incorporation of SrPI and, leading to a decrease of the cohesion forces within the polymers in the film matrix, making the films less resistant and stretchable (Liang et al., 2017).

3.2.4. *Light transmission, opacity and color of composite films*

UV–visible light barrier property reflects the potentiality of film to protect food against UV-radiation and slow the lipid oxidation (Hamdi et al., 2019; Hamdi, Nasri, Hajji, et al. (2019)). The transmission of UV and visible lights at selected wavelength (200–800 nm) of Cs100 film and composite films is investigated (Table S2). In the region of 200–280 nm, the Cs100 film had transmittance values below 23.7%, in agreement with data reported by Hamdi et al. (2019b) and Hamdi, Nasri, Hajji, et al. (2019). The Cs-SrPI films enriched with SrPI showed a significant inhibition of UV light transmission at 280–800 nm, which could be attributed to the added proteins promoting the creation of networks between the two polymers. It is interesting to note that the incorporation of SrPI improves the ability of chitosan films to block UV and visible light and the network was denser with SrPI incorporation (Prodpran, Benjakul, & Artharn, 2007). The transmission of UV light values at 280 nm of Cs90–10SrPI and Cs50–50SrPI films were 21.6% and 2.2%, respectively (Table S2). These findings are consistent with those of Batista et al. (2019) who found that myofibrillar fish proteins/chitosan composite films had a superior UV light barrier than chitosan film. It is thus concluded that SrPI has a strong light resistance, allowing for lesser visible light transmission in composite films.

The opacity of films, especially those used to cover food surfaces, is a crucial attribute to consider when defining their visual appearance. Table 2 shows that the opacity value of the composite films increases consistently with the increase of SrPI content, showing that the composite films were less transparent. The addition of 10% of SrPI increased 3-fold the opacity of composite films in comparison with Cs100 films ($p < 0.05$). Similar trend was reported by Ma, Tang, Yang, and Yin (2013) who found that the kidney bean protein isolate (KPI)-chitosan blend films became opaque with increase of KPI content. The same alterations were reported by Prodpran et al. (2007), who suggested that the rise in opacity may be due to intermolecular crosslinking between chitosan and proteins.

The color of films is of prime importance for different applications like food packaging (Abdelhedi et al., 2018). The rectangular coordinates (L*, a*, and b*) and color difference (ΔE) data of Cs-SrPI composite films are shown in Table 2. There is no significant change in lightness (L*) values ($P > 0.05$) between the various films. Cs100 film was transparent without any color. With the SrPI incorporation, the composite films became pale yellow and yellowish brown (higher values of b* and ΔE), and the intensity increased with the SrPI content. These

Table 2
Opacity and color values of the Cs-SrPI films.

Film	Opacity	*L**	*a**	*b**	*ΔE*
Cs 100	0.98 ± 0.08[a]	29.35 ± 0.18	-0.1 ± 0.01	-0.68 ± 0.03	–
Cs90–10SrPI	3.27 ± 0.11[b]	30.24 ± 0.26	-1.28 ± 0.09	2.81 ± 0.05	3.70 ± 0.11
Cs80–20SrPI	3.63 ± 0.03[c]	33.45 ± 0.08	-1.24 ± 0.02	4.55 ± 0.09	7.36 ± 0.10
Cs70–30SrPI	3.8 ± 0.07[d]	34.74 ± 0.19	-1.30 ± 0.01	5.18 ± 0.02	8.06 ± 0.01
Cs60–40SrPI	4.14 ± 0.05[e]	35.39 ± 0.10	-1.21 ± 0.00	5.32 ± 0.04	8.07 ± 0.09
Cs50–50SrPI	4.3 ± 0,13[f]	34.05 ± 0.67	-1.39 ± 0.07	6.14 ± 0.05	8.38 ± 0.49

findings present the same trend reported by Samsalee & Sothornvit (2019).

3.2.5. *Fourier transform infrared (FTIR) spectroscopy*

Fig. 1A shows the FTIR spectra of Cs100 and Cs-SrPI composite films in the wavenumber range of 800–4000 cm^{-1}. The FTIR spectrum of Cs100 film presents the characteristic bands of chitosan at 3281 cm^{-1}, 2920 cm^{-1}, 1549 cm^{-1}, 1409 cm^{-1}, 1152 cm^{-1} and 1071–1027 cm^{-1} assigned to the –OH and –N-H, -C-H, amide II (-NH_2 bending), amide III (C-N and N-H of amide bending), -C-N and glycosidic cycles (–C-O-C- bending), respectively (Habiba et al., 2017; Rahmi, Lelifajri, Julinawati & Shabrina, 2017).

Changes are observed on the FTIR spectra of composite films as shown in Fig. 1A. Indeed, it is interesting to note that the amide-I (1636 cm^{-1}) appeared only for composite films with high SrPI concentrations (30%, 40% and 50%, w/w polymer). In contrast, no shift is observed in the amide-II band (1549 cm^{-1}). Furthermore, the amide-III band shows a shift from 1409 cm^{-1} for Cs100 to a lower wavenumber (1406 cm^{-1}) in composite films. These changes are indicative of the alteration of the secondary structure of SrPI chains caused by strong interaction between Cs and proteins, presumably through hydrogen bonding between the functional groups of SrPI and the hydroxyl and

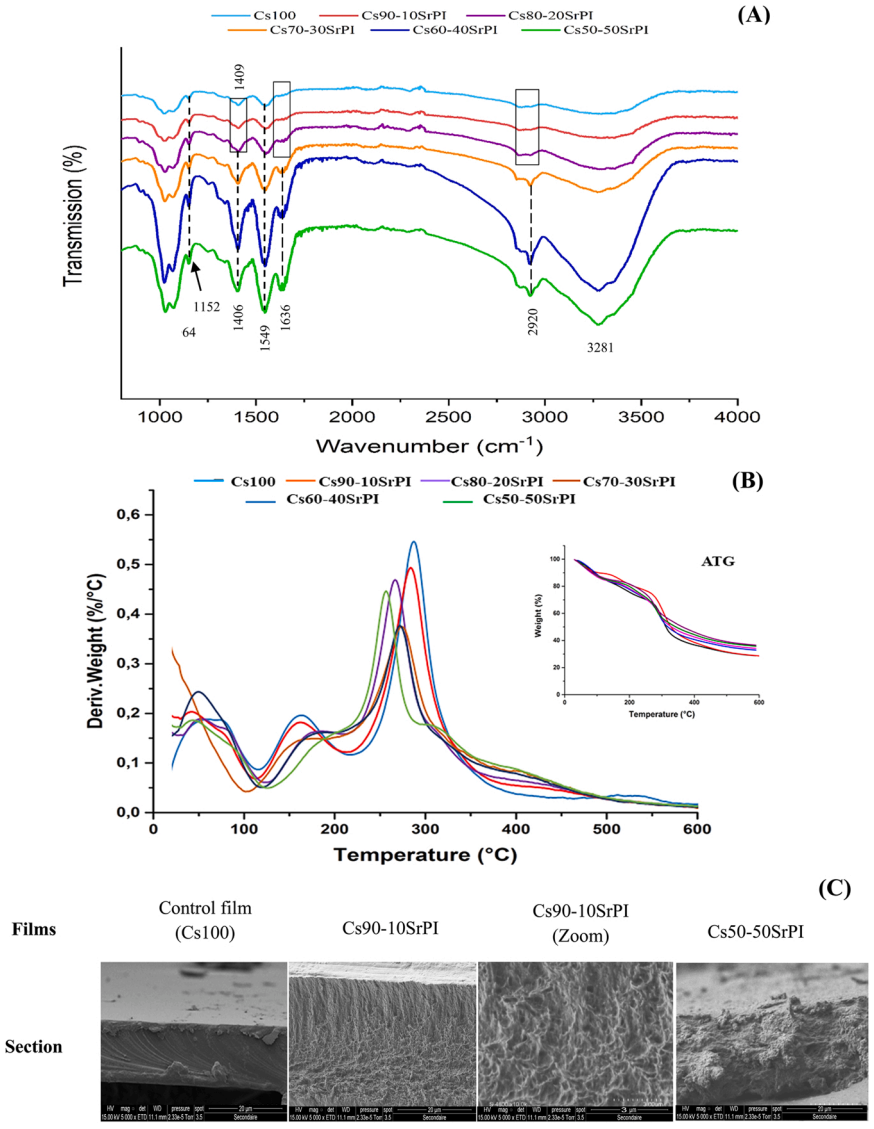

Fig. 1. FT-IR spectra (A), thermal properties (TGA and DTG thermograms) (B) and SEM micrographs (control film (Cs100) (20 μm); Cs90–10SrPI film (3 μm) and Cs50–50SrPI film (20 μm) for the cross-section observations (C)) of Cs-SrPI composite films.

amino groups of chitosan (Hajji et al., 2021).

3.2.6. Thermogravimetric analysis (TGA)

The thermal behaviors of Cs100 and Cs-SrPI composite films were studied and the results are illustrated in TGA and derivative thermogravimetric (DTG) thermograms (Fig. 1B).

The TGA profile of Cs100 was characterized by two main weight loss phases (Fig. 1B). The first phase occurred from 51 °C to 118 °C, corresponding to the elimination of water and volatile materials in the film such as acetic acid and glycerol (Liu, Xie, Yu, Chen & Li, 2009). The second phase was observed between 267 °C and 375 °C, with T_{max} (temperature, at which sample lost maximum of its weight) of about 300 °C, which is attributed to the decomposition of chitosan matrix.

It is obvious that the thermal degradation profile of the various films presented slight changes with the incorporation of SrPI. Indeed, when SrPI was added to the chitosan films, the T_{max} slightly decreased, showing that chitosan film had greater thermal stability than composite films. Andonegi et al. (2020) observed the similar trend in the case of chitosan/gelatin films.

3.2.7. Microstructure

Based on the structural and thermogravimetric data, Cs100, Cs90–10SrPI and Cs50–50SrPI films were selected for further analysis. Hence, SEM was performed to depict changes in the microstructure of the selected films (Fig. 1**C**). The SEM images reveal visible differences between composite and control films. Cs100 film cross-section appeared smooth, homogeneous, uniform and without cracks (Fig. 1C), in agreement with observations made by Kaya et al. (2018) and Zhang et al. (2016). Moreover, Cs90–10SrPI film had a uniform and slightly rigid structure with few pores. The observed structure may be explained by effective cross-linking of SrPI and Cs, which increases the number of hydrophilic groups on the surface of films (Zhang et al., 2019). Films prepared with high content of SrPI (50%, w/w polymer) showed a heterogeneous structure with apparent agglomerates , in which SrPI was entrapped in the continuous network of chitosan. This was probably due to the agglomeration of protein isolate (Ferreira, Nunes, Delgadillo & Lopes-da-Silva, 2009). In fact, the addition of SrPI in the film-forming matrix influenced intramolecular and intermolecular hydrogen bonding as well as physical interactions between Cs and glycerol, leading to heterogeneous and resulting in the irregular rough microstructure of the films (Rui et al., 2017).

3.3. Biological activities

3.3.1. Antioxidant properties of composite films

The DPPH radical scavenging activity, reducing power, ferrous ion-chelating activity, and β-carotene bleaching test were used to assess the antioxidant properties of Cs100 and Cs-SrPI films.

As illustrated in Table 1, Cs100 film exhibited moderate DPPH scavenging (74%) and chelating activities (36%) and low reducing power of $OD_{700} = 0.165$. It's worth mentioning that adding SrPI to the chitosan matrix considerably increased the antioxidant capacity of composite films in a dose-dependent manner ($p < 0.05$). This finding might be attributed to the antioxidant potential of SrPI (Table 1). The highest DPPH radical scavenging potential, ferrous ion-chelating activity and reducing power were obtained with Cs50–50SrPI film, reaching values of 100%, 84% and $OD_{700} = 0.894$, respectively. Antioxidant activities were enhanced even at a low concentration of SrPI (10%) as compared to control film, suggesting that SrPI might be used as an antioxidant.

The antioxidant activity of films was also assessed by β-carotene bleaching assay. Table 1 demonstrates that the addition of SrPI to the Cs film led to a significant improvement in the activity. In fact, the Cs50–50SrPI film inhibited β-carotene bleaching by 54%, compared to 23% for Cs100 film. Our data are in agreement with those of Hamdi et al. (2019) and Hamdi, Nasri, Hajji, et al. (2019) who reported that the increase of cartenoproteins content in the chitosan matrix enhanced the antioxidant activity of blended films.

3.3.2. Antibacterial potential of composite films

The antibacterial potential of the prepared films was evaluated against five Gram-negative and four Gram-positive pathogenic strains by the agar well diffusion method. The results in Table S3 revealed that the films were effective against all bacteria tested and that this effect differed depending on the target strain as well as the SrPI content. In fact, Gram-positive bacteria were significantly more inhibited than Gram-negative strains, particularly for *L. monocytogenes* , *M. luteus* and *B. cereus*, while the lowest effect was obtained against the Gram-positive strain *S. aureus* for all samples.

For all microbial strains tested in this study, all film samples were efficient in preventing microorganism development (Table S3). Chitosan presents outstanding antimicrobial activity. The control film (Cs100) exhibited inhibition zones with diameters of 10.10 mm for *S. aureus*, 13.76 mm for *L. monocytogenes*, 13.76 mm for *M. luteus*, 12.50 mm for *B. aureus*, 11.65 mm for *S. enterica*, 11.45 mm for *P. aeruginosa*, 11.85 mm for *Enterobacter. sp*, 13.55 mm for *E. coli* and 13.75 mm for *K. pneumoniae*. SrPI incorporation into the Cs matrix resulted in a slight decrease in antibacterial efficacy against all tested microbiological strains, which was dependent on the SrPI content (Table S3). Nevertheless, composite films exhibited acceptable antimicrobial properties, and could be used in the development of edible coatings and films for food packaging applications.

3.4. Effect of Cs100 and Cs-SrPI packaging on shrimp preservation

One of the strategies described to increase food preservation is packaging with edible biofilms (Costa, Maciel, Teixeira, Vicente & Cerqueira, 2018). In this context, Cs90–10SrPI and Cs50–50SrPI were employed to cover the surface of the shrimp, as compared to the control packing (Cs100). The moisture of the unpackaged pieces of shrimp was constant of about 26% during storage. The incorporation of SrPI into the chitosan film matrix resulted in a slight increase in the moisture content of packaged shrimp after 9 days storage at 4 °C, as shown in Table 3. For example, SH-1 showed an increase in moisture content from 27.30% at day 0–28.78% at day 9.

Results in Table 3 showed that the pH value of non-packaged (SH-C) and packaged shrimp samples (SH-1, SH-2, SH-3) gradually increased during the 9 days of cold storage from 7.42 to 7.91, 7.05–7.52, 6.81–7.13 and 6.41–6.89, respectively ($p < 0.05$). The most important reason of the increased pH is the accumulation of nitrogen compounds derived from the microbial action (Arancibia, Alemán, López-Caballero, Gómez-Guillén & Montero, 2015; Kakaei & Shahbazi, 2016). An increase in pH indicates that the shrimps begin to putrefy (Sf et al., 2008). On day 9, the pH value of the packaged samples was much lower than that of the SH-C sample, indicating that the wrapped shrimps were better preserved. Interestingly, the use of Cs100 and Cs-SrPI films to wrap the shrimp can help reduce pH changes and extend the shelf life of the shrimp. The same trend was reported by Mohebi & Shahbazi (2016).

The appearance and color of the shrimp are shown in Fig. 2. The color of the control and packaged shrimps changed from gray to yellowish after 9 days of storage. It seems that the packaging with Cs and Cs-SrPI films had little effect on the color changes shrimps.

In general, lipid oxidation is triggered during the storage and processing of crustaceans. The peroxide value (PV) is widely determined to investigate the detection of fatty acid hydroperoxides as main lipid oxidation products (Chaijan, 2011). Fig. 3A shows the PV changes of treated shrimp with different packaging films through a refrigerated storage period of 9 days. A significant increase of PV with the storage time was observed in non-packaged shrimps from 0.0108 to 0.0313 meq/kg lipid ($p < 0.05$). The PV values of non-packaged shrimps were substantially higher ($p < 0.05$) than those of packaged shrimps. In fact, the PV values of SH-1, SH-2, and SH-3 were 0.0197,

Table 3
Changes in pH, moisture parameters and microbial parameters (TPF: total psychrotrophic flora, TMF: total mesophilic flora) of shrimp samples at 0, 3, 6 and 9 days of storage.

Parameter	Day	SH-C	SH-1	SH-2	SH-3
Moisture Content	0	26.19 ± 0.10^{aA}	27.30 ± 0.14^{Ab}	28.08 ± 0.02^{Ac}	28.25 ± 0.03^{aD}
	3	26.30 ± 0.70^{aA}	27.56 ± 0.06^{bB}	28.92 ± 0.06^{bC}	$29.61 \pm 0.08b^{dD}$
	6	26.50 ± 0.56^{aA}	27.75 ± 0.35^{aB}	28.21 ± 0.30^{bAB}	28.74 ± 0.05^{Bc}
	9	26.77 ± 0.53^{aA}	28.78 ± 0.04^{abB}	28.59 ± 0.55^{cB}	29.30 ± 0.33^{cB}
pH	0	7.42 ± 0.06^{dA}	7.05 ± 0.06^{dB}	6.81 ± 0.02^{dC}	6.41 ± 0.02^{dD}
	3	7.62 ± 0.03^{cA}	7.20 ± 0.02^{cB}	6.92 ± 0.01^{cC}	6.58 ± 0.04^{cD}
	6	7.73 ± 0.05^{bA}	7.41 ± 0.01^{bB}	7.01 ± 0.03^{bC}	6.77 ± 0.04^{bD}
	9	7.91 ± 0.08^{aA}	7.52 ± 0.02^{aB}	7.13 ± 0.01^{aC}	6.89 ± 0.02^{aD}
TPF (log CFU/g)	0	0.21 ± 0.006^{dD}	–	–	–
	3	0.52 ± 0.005^{cD}	0.05 ± 0.003^{cC}	0.02 ± 0.00^{cB}	0.01 ± 0.003^{cA}
	6	1.07 ± 0.002^{bC}	0.68 ± 0.02^{bC}	0.52 ± 0.002^{bB}	0.35 ± 0.004^{bA}
	9	2.21 ± 0.008^{aD}	1.16 ± 0.01^{aC}	0.65 ± 0.004^{aB}	0.49 ± 0.02^{aA}
TMF (log CFU/g)	0	0.32 ± 0.006^{dD}	–	–	–
	3	0.66 ± 0.006^{cD}	0.48 ± 0.004^{cC}	0.31 ± 0.004^{cB}	0.26 ± 0.01^{cA}
	6	3.44 ± 0.006^{bC}	0.58 ± 0.008^{bC}	0.40 ± 0.006^{bB}	0.29 ± 0.004^{bA}
	9	5.79 ± 0.006^{aD}	1.2 ± 0.006^{aC}	0.58 ± 0.008^{aB}	0.44 ± 0.01^{aA}

SH-C: control shrimp (unpackaged) with no treatment; **SH-1**: shrimp packaged with Cs100 film; **Sh-2**: shrimp packaged with Cs90-10SrPI film; **Sh-3**: shrimp packaged with Cs50-50SrPI film. (**a–d**) Different letters in each column mean a significant difference for same samples on different days of storage ($p < 0.05$). (**A–D**) Different letters indicate significant differences between samples on same day of storage ($p < 0.05$).

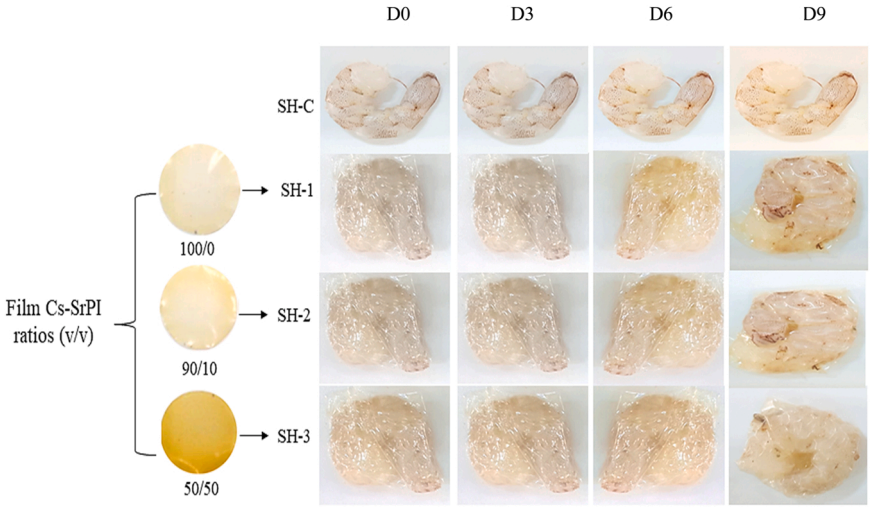

Fig. 2. Color changes of packaged shrimps.

0.0177, and 0.0157 meq/kg lipid at day 9, respectively ($p < 0.05$). The higher the SrPI content, the lower the PV of packaged shrimps. The significant PV increase could be explained by the release of fatty acid products, which are highly susceptible to oxidation and thus form unstable lipid hydroperoxides (Nirmal & Benjakul, 2011).

Therefore, the bioactive component SrPI has been shown to effectively slow the production of specific oxidation products in refrigerated shrimp. The increase in free fatty acids was very sensitive to oxidation and produced unstable lipid hydroperoxides, which were then degraded to shorter chain hydrocarbons such as aldehydes.

TBARS test was used to evaluate the formation of secondary oxidation products during 9 days storage at 4 °C (Benjakul, Visessanguan, Phongkanpai & Tanaka, 2005), as shown in Fig. 3B. The control shrimps SH-C initially had a TBARS value of 2.17 mg MDA/kg ($P < 0.05$), which gradually increased to 4.36 mg MDA/kg after 9 days storage ($P < 0.05$). The incorporation of SrPI in the chitosan film induced a decrease in the TBARS formation. The TBARS of SH-1, SH-2 and SH-3 reached 3.03, 2.05 and 1.84 mg MDA/kg on day 9, respectively ($P < 0.05$). The loss of water from the samples and the increase in the degree of oxidation of polyunsaturated fatty acids are most likely the two major reasons for the substantial increase in TBARS level during storage (Balti et al., 2020). It's worthy to note that the addition of SrPI to the chitosan film was effective to prevent the passage of oxygen, water molecules and other volatile compounds, thereby reducing the lipid peroxidation. According to Yildiz (2015), seafood products with a TBARS content below 5 mg MDA/kg are estimated to be of good quality. Our findings demonstrated that the TBARS level of both unpackaged and packaged shrimps did not surpass the lower reference (5 mg MDA/kg), indicating that the shrimps were safe to eat.

Lipid oxidation was also estimated by the measurement of conjugated dienes (CD) content. The results showed an increase in CD value of all samples during storage (Fig. 3C). In fact, the highest CD values were obtained in SH-C and SH-1, reaching $OD_{233\ nm}$ values of 0.304 and 0.222 on day 9, respectively. Interestingly, SH-2 and SH-3 had the lowest $OD_{233\ nm}$ values of 0.208 and 0.198 ($p < 0.05$), respectively, indicating that composite packaging film successfully reduced the CD formation. Therefore, SrPI could be considered as an interesting antioxidant additive that can prevent food oxidation.

One of the most important factors for determining the quality of seafood is the microbial count. Table 3 shows the changes of total psychrophilic flora (TPF) and mesophilic flora (TMF) in packaged shrimps during refrigerated storage. The total viable counts of all the shrimps increased continuously with the storage time ($P < 0.05$). The TPF and TMF of control sample increased from 0.21 and 0.32 log CFU/g at day

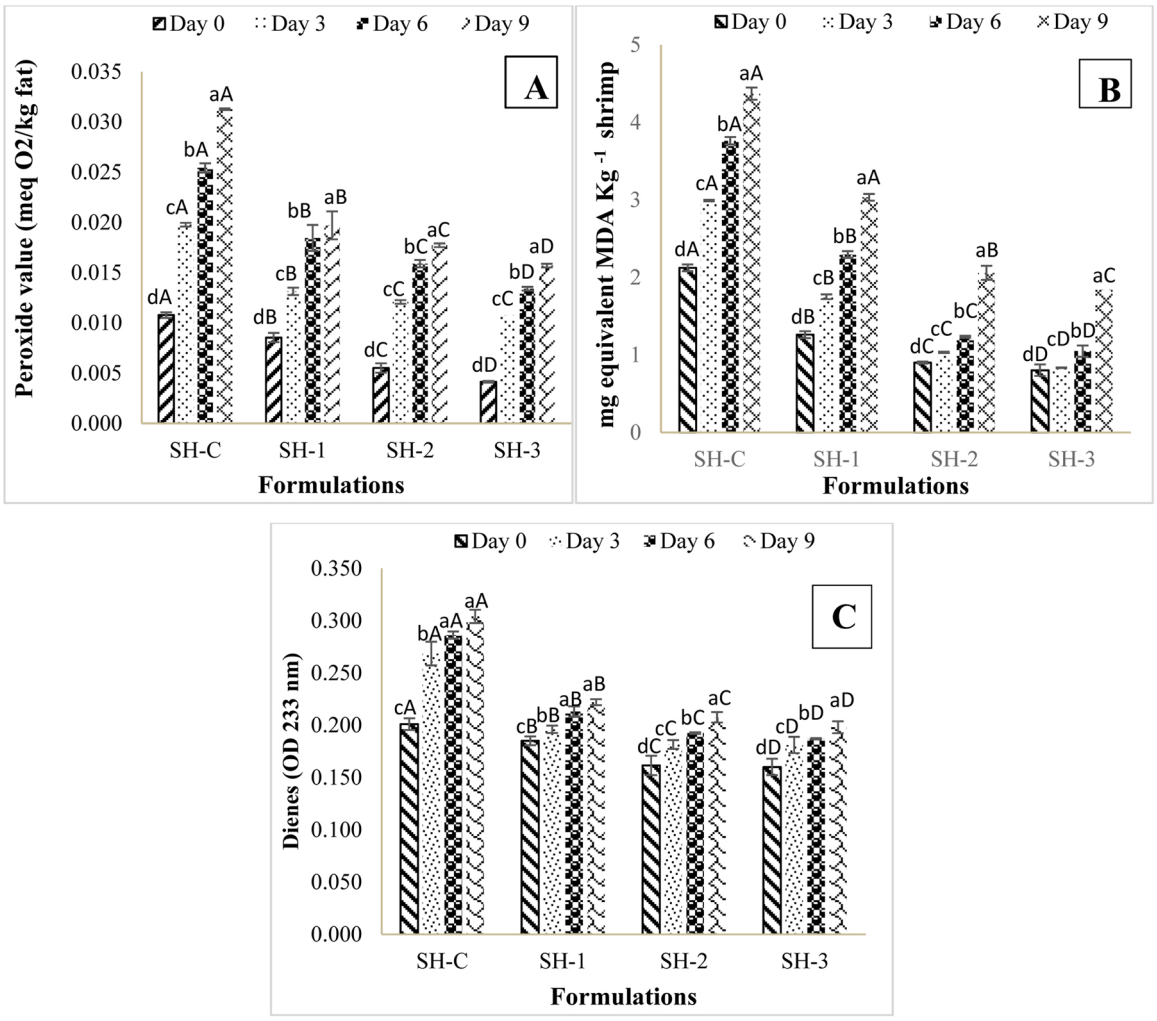

Fig. 3. Effect of SrPI incorporation (10% and 50%, w/w polymer) in the chitosan film matrix (Cs100) on thiobarbituric-acid reactive substances (TBARS, mg MDA/kg) (A), peroxide value (m eq O2/kg fat) (B) and conjugated dienes values (OD 233 nm) of packaged shrimps during refrigerated period (C).
(a-d) Different letters in each column mean a significant difference for the same sample on different storage days ($p < 0.05$). (A–D) Different letters indicate significant differences between samples on the same storage day ($p < 0.05$).

0 to 2.21 and 5.79 log CFU/g at day 9, respectively, which are below the maximal permissible limit for acceptable quality of shrimp meat (Mohebi & Shahbazi, 2016). Table 3 shows that the TPF and TMF of SH2 and SH-3 were considerably lower than those of SH-C and SH-1 ($P < 0.05$). These findings imply that SrPI can effectively inhibit the development of microorganisms and extend the shelf life of shrimps.

4. Conclusion

Composite films were prepared from two biopolymers, *i.e* SrPI and Cs derived from sardinella and blue crab by-products, respectively. The physico-chemical and antioxidant characteristics of SrPI were studied, and the results reveal that it may be used as a source of proteins. Composite films were prepared by incorporation of SrPI to the chitosan film matrix at different contents, and characterized using various techniques. The barrier (water vapor and UV), microstructural, opacity, antioxidant and antibacterial properties of composite films are considerably improved as compared to the control film. Thermal, spectroscopic, and microstructural analyses allowed to prove the compatibility of the two biopolymers. Regarding their interesting biological activities, the Cs-SrPI composite films improve the microbial stability and reduce the lipid peroxidation of wrapped shrimps during cold storage. Therefore, it is concluded that the blend of chitosan and SrPI could be very promising alternative to develop active packaging food.

Youssra Ben Azaza: Conceptualization, Methodology, Investigation, Validation, Formal analysis, Visualization, Writing – original draft. **Marwa Hamdi:** Investigation, Methodology. **Christophe Charmette:** Investigation, Methodology. **Mourad jridi:** Investigation. **Suming Li:** Funding acquisition, Supervision, Writing – review & editing. **Moncef Nasri:** Supervision, Editing, Validation. **Rim Nasri:** Resources, Supervision, Funding acquisition, Writing – review & editing.

Acknowledgments

This research work was funded by the Ministry of Higher Education and Scientific Research, Tunisia (grant No. 18PJEC08/01), and by the

joint French-Tunisian PHC Utique Program (grant No: 19G0815).

References

Abdelhedi, O., Nasri, R., Jridi, M., Kchaou, H., Nasreddine, B., Karbowiak, T., … Nasri, M. (2018). Composite bioactive films based on smooth-hound viscera proteins and gelatin: physicochemical characterization and antioxidant properties. *Food Hydrocolloids, 74*, 176–186. https://doi.org/10.1016/j.foodhyd.2017.08.006

Andonegi, M., Heras, K. L., Santos-Vizcaíno, E., Igartua, M., Hernandez, R. M., de la Caba, K., & Guerrero, P. (2020). Structure-properties relationship of chitosan/collagen films with potential for biomedical applications. *Carbohydrate Polymers, 237*, Article 116159. https://doi.org/10.1016/j.carbpol.2020.116159

Anuar, H., Izzati, A., Inani, S., E'zzati, M., Salimah, A., Ali, F., & Manshor, M. R. (2017). Impregnation of cinnamon essential oil into plasticised polylactic acid biocomposite film for active food packaging. *Journal of Packaging Technology and Research*. https://doi.org/10.1007/s41783-017-0022-1

AOAC (2000). Official Methods of Analysis of AOAC International, 17th Edition Z423645. Sigma-Aldrich. Retrieved from ⟨https://www.sigmaaldrich.com/catalog/product/aldrich/z423645⟩ (Accessed 11 April 2021).

Arancibia, M. Y., Alemán, A., López-Caballero, M. E., Gómez-Guillén, M. C., & Montero, P. (2015). Development of active films of chitosan isolated by mild extraction with added protein concentrate from shrimp waste. *Food Hydrocolloids, 43*, 91–99. https://doi.org/10.1016/j.foodhyd.2014.05.006

Balti, R., Ben Mansour, M., Zayoud, N., Le Balc'h, R., Brodu, N., Arhaliass, A., & Massé, A. (2020). Active exopolysaccharides based edible coatings enriched with red seaweed (Gracilaria gracilis) extract to improve shrimp preservation during refrigerated storage. *Food Bioscience, 34*, Article 100522. https://doi.org/10.1016/j.fbio.2019.100522

Batista, J. T. S., Araújo, C. S., Peixoto Joele, M. R. S., Silva, J. O. C., & Lourenço, L. F. H. (2019). Study of the effect of the chitosan use on the properties of biodegradable films of myofibrillar proteins of fish residues using response surface methodology. *Food Packaging and Shelf Life*. ⟨https://agris.fao.org/agris-search/search.do?recordID=US201900208062⟩.

Benjakul, S., Visessanguan, W., Phongkanpai, V., & Tanaka, M. (2005). Antioxidative activity of caramelisation products and their preventive effect on lipid oxidation in fish mince. *Food Chemistry, 90*(1), 231–239. https://doi.org/10.1016/j.foodchem.2004.03.045

Bersuder, P., Hole, M., & Smith, G. (1998). Antioxidants from a heated histidine-glucose model system. I: Investigation of the antioxidant role of histidine and isolation of antioxidants by high-performance liquid chromatography. *Journal of the American Oil Chemists' Society, 75*(2), 181–187. https://doi.org/10.1007/s11746-998-0030-y

Buege, J. A., & Aust, S. D. (1972). On the solubilization of NADPH-cytochrome c reductase from rat liver microsomes with crude pancreatic lipase. *Biochimica et Biophysica Acta ((BBA)) – General Subjects, 286*(2), 433–436. https://doi.org/10.1016/0304-4165(72)90284-X

Chaijan, M. (2011). Physicochemical changes of tilapia (Oreochromis niloticus) muscle during salting. *Food Chemistry, 129*(3), 1201–1210. https://doi.org/10.1016/j.foodchem.2011.05.110

Cho, S.-J. (2020). Changes in the antioxidant properties of rice bran protein isolate upon simulated gastrointestinal digestion. *LWT, 126*, Article 109206. https://doi.org/10.1016/j.lwt.2020.109206

Coltelli, M., Wild, F., Bugnicourt, E., Cinelli, P., Lindner, M., Schmid, M., … Lazzeri, A. (2015). State of the art in the development and properties of protein-based films and coatings and their applicability to cellulose based products: an extensive review. *Coatings, 6*. https://doi.org/10.3390/coatings6010001

Costa, M. J., Maciel, L. C., Teixeira, J. A., Vicente, A. A., & Cerqueira, M. A. (2018). Use of edible films and coatings in cheese preservation: opportunities and challenges. *Food Research International, 107*, 84–92. https://doi.org/10.1016/j.foodres.2018.02.013

Decker, E. A., & Welch, B. (1990). Role of ferritin as a lipid oxidation catalyst in muscle food. *Journal of Agricultural and Food Chemistry* (University of K.) ⟨https://agris.fao.org/agris-search/search.do?recordID=US9130072⟩.

Duan, J., Wu, R., Strik, B. C., & Zhao, Y. (2011). Effect of edible coatings on the quality of fresh blueberries (Duke and Elliott) under commercial storage conditions. *Postharvest Biology and Technology, 59*(1), 71–79. https://doi.org/10.1016/j.postharvbio.2010.08.006

Ferreira, C. O., Nunes, C. A., Delgadillo, I., & Lopes-da-Silva, J. A. (2009). Characterization of chitosan–whey protein films at acid pH. *Food Research International, 42*(7), 807–813. https://doi.org/10.1016/j.foodres.2009.03.005

García, F. T., & Sobral, P. J. do A. (2005). Effect of the thermal treatment of the filmogenic solution on the mechanical properties, color and opacity of films based on muscle proteins of two varieties of Tilapia. *LWT – Food Science and Technology, 38*(3), 289–296. https://doi.org/10.1016/j.lwt.2004.06.002

Gennadios, A., Handa, A., Froning, G. W., Weller, C. L., & Hanna, M. A. (1998). Physical properties of egg white–dialdehyde starch films†. *Journal of Agricultural and Food Chemistry, 46*(4), 1297–1302. https://doi.org/10.1021/jf9708047

Habiba, U., Joo, T. C., Siddique, T. A., Salleh, A., Ang, B. C., & Afifi, A. M. (2017). Effect of degree of deacetylation of chitosan on adsorption capacity and reusability of chitosan/polyvinyl alcohol/TiO2 nano composite. *International Journal of Biological Macromolecules, 104*(Pt A), 1133–1142. https://doi.org/10.1016/j.ijbiomac.2017.07.007

Hajji, S., Kchaou, H., Bkhairia, I., Ben Slama-Ben Salem, R., Boufi, S., Debeaufort, F., & Nasri, M. (2021). Conception of active food packaging films based on crab chitosan and gelatin enriched with crustacean protein hydrolysates with improved functional and biological properties. *Food Hydrocolloids, 116*, Article 106639. https://doi.org/10.1016/j.foodhyd.2021.106639

Hamdi, M., Feki, A., Bardaa, S., Li, S., Nagarajan, S., Mellouli, M., … Nasri, R. (2020). A novel blue crab chitosan/protein composite hydrogel enriched with carotenoids endowed with distinguished wound healing capability: in vitro characterization and in vivo assessment. *Materials Science and Engineering: C, 113*, Article 110978. https://doi.org/10.1016/j.msec.2020.110978

Hamdi, M., Hajji, S., Affes, S., Taktak, W., Maâlej, H., Nasri, M., & Nasri, R. (2018). Development of a controlled bioconversion process for the recovery of chitosan from blue crab (Portunus segnis) exoskeleton. *Food Hydrocolloids, 77*, 534–548. https://doi.org/10.1016/j.foodhyd.2017.10.031

Hamdi, M., Nasri, R., Amor, I. B., Li, S., Gargouri, J., & Nasri, M. (2020). Structural features, anti-coagulant and anti-adhesive potentials of blue crab (Portunus segnis) chitosan derivativeS: Study of the effects of acetylation degree and molecular weight. *International Journal of Biological Macromolecules, 160*, 593–601. https://doi.org/10.1016/j.ijbiomac.2020.05.246

Hamdi, M., Nasri, R., Hajji, S., Nigen, M., Li, S., & Nasri, M. (2019). Acetylation degree, a key parameter modulating chitosan rheological, thermal and film-forming properties. *Food Hydrocolloids, 87*, 48–60. https://doi.org/10.1016/j.foodhyd.2018.07.027

Hamdi, M., Nasri, R., Li, S., & Nasri, M. (2019). Bioactive composite films with chitosan and carotenoproteins extract from blue crab shells: biological potential and structural, thermal, and mechanical characterization. *Food Hydrocolloids, 89*, 802–812. https://doi.org/10.1016/j.foodhyd.2018.11.062

Hosseini, S. F., Rezaei, M., Zandi, M., & Ghavi, F. F. (2013). Preparation and functional properties of fish gelatin–chitosan blend edible films. *Food Chemistry, 136*(3), 1490–1495. https://doi.org/10.1016/j.foodchem.2012.09.081

Jridi, M., Hajji, S., Ayed, H. B., Lassoued, I., Mbarek, A., Kammoun, M., … Nasri, M. (2014). Physical, structural, antioxidant and antimicrobial properties of gelatin–chitosan composite edible films. *International Journal of Biological Macromolecules, 67*, 373–379. https://doi.org/10.1016/j.ijbiomac.2014.03.054

Kakaei, S., & Shahbazi, Y. (2016). Effect of chitosan-gelatin film incorporated with ethanolic red grape seed extract and Ziziphora clinopodioides essential oil on survival of Listeria monocytogenes and chemical, microbial and sensory properties of minced trout fillet. *LWT – Food Science and Technology, 72*. https://doi.org/10.1016/j.lwt.2016.05.021

Kaya, M., Ravikumar, P., Ilk, S., Mujtaba, M., Akyuz, L., Labidi, J., … Erkul, S. K. (2018). Production and characterization of chitosan based edible films from Berberis crataegina's fruit extract and seed oil. *Innovative Food Science & Emerging Technologies, 45*, 287–297. https://doi.org/10.1016/j.ifset.2017.11.013

Koleva, I. I., van Beek, T. A., Linssen, J. P. H., de Groot, A., & Evstatieva, L. N. (2002). Screening of plant extracts for antioxidant activity: a comparative study on three testing methods. *Phytochemical Analysis: PCA, 13*(1), 8–17. https://doi.org/10.1002/pca.611

Kumarakuru, K., Reddy, C. K., & Haripriya, S. (2018). Physicochemical, morphological and functional properties of protein isolates obtained from four fish species. *Journal of Food Science and Technology, 55*(12), 4928–4936. https://doi.org/10.1007/s13197-018-3427-0

Liang, C., Jia, M., Tian, D., Tang, Y., Ju, W., Ding, S., … Wang, X. (2017). Edible sturgeon skin gelatine films: tensile strength and UV light-barrier as enhanced by blending with esculine. *Journal of Functional Foods, 37*, 219–228. https://doi.org/10.1016/j.jff.2017.07.051

Li, K., Jin, S., Liu, X., Chen, H., He, J., & Li, J. (2017). Preparation and Characterization of Chitosan/Soy Protein Isolate Nanocomposite Film Reinforced by Cu Nanoclusters. *Polymers, 9*(12), 247. https://doi.org/10.3390/polym9070247

Liu, H., Xie, F., Yu, L., Chen, L., & Li, L. (2009). Thermal processing of starch-based polymers. *Progress in Polymer Science, 34*(12), 1348–1368. https://doi.org/10.1016/j.progpolymsci.2009.07.001

Ma, W., Tang, C.-H., Yang, X.-Q., & Yin, S.-W. (2013). Fabrication and characterization of kidney bean (Phaseolus vulgaris L.) protein isolate–chitosan composite films at acidic pH. *Food Hydrocolloids, 31*(2), 237–247. https://doi.org/10.1016/j.foodhyd.2012.10.007

Mohan, C. O., Ravishankar, C. N., Lalitha, K. V., & Srinivasa Gopal, T. K. (2012). Effect of chitosan edible coating on the quality of double filleted Indian oil sardine (Sardinella longiceps) during chilled storage. *Food Hydrocolloids, 26*(1), 167–174. https://doi.org/10.1016/j.foodhyd.2011.05.005

Mohebi, E., & Shahbazi, Y. (2016). Application of chitosan and gelatin based active packaging films for peeled shrimp preservation: a novel functional wrapping design. *LWT – Food Science and Technology, 76*. https://doi.org/10.1016/j.lwt.2016.10.062

Nasri, R., Taktak, W., Hamdi, M., Ben Amor, N., Kabadou, A., Li, S., & Nasri, M. (2020). Sardinelle protein isolate as a novel material for oil microencapsulation: Novel alternative for fish by-products valorisation. *Materials Science and Engineering: C, 116*, Article 111164. https://doi.org/10.1016/j.msec.2020.111164

Nasri, R., Younes, I., Jridi, M., Trigui, M., Bougatef, A., Nedjar-Arroume, N., … Karra-Châabouni, M. (2013). ACE inhibitory and antioxidative activities of Goby (Zosterissessor ophiocephalus) fish protein hydrolysates: effect on meat lipid oxidation. *Food Research International, 54*(1), 552–561. https://doi.org/10.1016/j.foodres.2013.07.001

Niamsa, N., Morakot, N., & Baimark, Y. (2010). Water-vapor permeability of chitosan and methoxy poly(ethylene glycol)-b-poly(ε-caprolactone) blend homogeneous

films. *Water Properties in Food, Health, Pharmaceutical and Biological Systems: ISOPOW, 10*, 459–464. https://doi.org/10.1002/9780470958193.ch36

Nirmal, N. P., & Benjakul, S. (2011). Retardation of quality changes of Pacific white shrimp by green tea extract treatment and modified atmosphere packaging during refrigerated storage. *International Journal of Food Microbiology, 149*(3), 247–253. https://doi.org/10.1016/j.ijfoodmicro.2011.07.002

Oliyaei, N., Ghorbani, M., Moosavi-Nasab, M., Sadeghimahoonak, A. R., & Maghsoudloo, Y. (2017). Effect of temperature and alkaline pH on the physicochemical properties of the protein isolates extracted from the whole ungutted lanternfish (Benthosema pterotum). *Journal of Aquatic Food Product Technology, 26*(10), 1134–1143. https://doi.org/10.1080/10498850.2014.940564

Prodpran, T., Benjakul, S., & Artharn, A. (2007). Properties and microstructure of protein-based film from round scad (Decapterus maruadsi) muscle as affected by palm oil and chitosan incorporation. *International Journal of Biological Macromolecules, 41*(5), 605–614. https://doi.org/10.1016/j.ijbiomac.2007.07.020

Rahmi, Lelifajri, Julinawati, & Shabrina. (2017). Preparation of chitosan composite film reinforced with cellulose isolated from oil palm empty fruit bunch and application in cadmium ions removal from aqueous solutions. *Carbohydrate Polymers, 170*, 226–233. https://doi.org/10.1016/j.carbpol.2017.04.084

Rui, L., Xie, M., Hu, B., Zhou, L., Yin, D., & Zeng, X. (2017). A comparative study on chitosan/gelatin composite films with conjugated or incorporated gallic acid. *Carbohydrate Polymers, 173*, 473–481. https://doi.org/10.1016/j.carbpol.2017.05.072

Samsalee, N., & Sothornvit, R. (2019). Development and characterization of porcine plasma protein-chitosan blended films. *Food Packaging and Shelf Life, 22*, Article 100406. https://doi.org/10.1016/j.fpsl.2019.100406

Sf, H., Ro, M., Dd, B., Ac, D., Jm, E., Db, P., … J, K. (2008). The effect of pH on shelf-life of pork during aging and simulated retail display. *Meat Science, 82*(1), 86–93. https://doi.org/10.1016/j.meatsci.2008.12.008

Shantha, N. C., & Decker, E. A. (1993). Conjugated linoleic acid concentrations in processed cheese containing hydrogen donors, iron and dairy-based additives. *Food Chemistry, 47*(3), 257–261. https://doi.org/10.1016/0308-8146(93)90158-C

Shen, X. L., Wu, J. M., Chen, Y., & Zhao, G. (2010). Antimicrobial and physical properties of sweet potato starch films incorporated with potassium sorbate or chitosan. *Food Hydrocolloids, 24*(4), 285–290. https://doi.org/10.1016/j.foodhyd.2009.10.003

Souza, B., Cerqueira, M., Ruiz, H., Martins, J., Casariego, A., Teixeira, J., & Vicente, A. (2010). Effect of chitosan-based coatings on the shelf life of salmon (Salmo salar). *Journal of Agricultural and Food Chemistry, 58*. https://doi.org/10.1021/jf102366k

Srinivasan, M., Holl, F. B., & Petersen, D. J. (2011). Influence of indoleacetic-acid-producing Bacillus isolates on the nodulation of Phaseolus vulgaris by Rhizobium etli under gnotobiotic conditions. *Canadian Journal of Microbiology*. https://doi.org/10.1139/m96-129

Taktak, W., Nasri, R., Lopez-Rubio, A., Hamdi, M., Gomez-Mascaraque, L. G., Ben Amor, N., … Karra-chaâbouni, M. (2019). Improved antioxidant activity and oxidative stability of spray dried European eel (Anguilla anguilla) oil microcapsules: effect of emulsification process and eel protein isolate concentration. *Materials Science and Engineering: C, 104*, Article 109867. https://doi.org/10.1016/j.msec.2019.109867

Van Den Berghe, D. A., Ieven, M., Mertens, F., & Vlietinck, A. J. (1978). Screening of higher plants for biological activities. II. Antiviral activity. *Lloydia, 41*(5), 463–471.

van den Broek, L. A. M., Knoop, R. J. I., Kappen, F. H. J., & Boeriu, C. G. (2015). Chitosan films and blends for packaging material. *Carbohydrate Polymers, 116*, 237–242. https://doi.org/10.1016/j.carbpol.2014.07.039

Volpe, M. G., Siano, F., Paolucci, M., Sacco, A., Sorrentino, A., Malinconico, M., & Varricchio, E. (2015). Active edible coating effectiveness in shelf-life enhancement of trout (Oncorhynchusmykiss) fillets. *LWT – Food Science and Technology, 60*(1), 615–622. https://doi.org/10.1016/j.lwt.2014.08.048

Yang, T.-L. (2011). Chitin-based Materials in Tissue Engineering: Applications in Soft Tissue and Epithelial Organ. *Int. J. Mol. Sci., 12*(3), 1936–1963. https://doi.org/10.3390/ijms12031936

Yildirim, A., Mavi, A., & Kara, A. A. (2001). Determination of antioxidant and antimicrobial activities of Rumex crispus L. extracts. *Journal of Agricultural and Food Chemistry, 49*(8), 4083–4089. https://doi.org/10.1021/jf0103572

Yildiz, P. O. (2015). Effect of essential oils and packaging on hot smoked rainbow trout during storage. *Journal of Food Processing and Preservation, 39*(6), 806–815. https://doi.org/10.1111/jfpp.12291

Zhang, W., Chen, J., Chen, Y., Xia, W., Xiong, Y. L., & Wang, H. (2016). Enhanced physicochemical properties of chitosan/whey protein isolate composite film by sodium laurate-modified TiO2 nanoparticles. *Carbohydrate Polymers, 138*, 59–65. https://doi.org/10.1016/j.carbpol.2015.11.031

Zhang, L., Liu, Z., Wang, X., Dong, S., Sun, Y., & Zhao, Z. (2019). The properties of chitosan/zein blend film and effect of film on quality of mushroom (Agaricus bisporus). *Postharvest Biol. Technol., 155*, 47–56. https://doi.org/10.1016/j.postharvbio.2019.05.013